ACS Catalysis

Research Article

pubs.acs.org/acscatalysis

Aqueous Phase Hydroalkylation and Hydrodeoxygenation of Phenol by Dual Functional Catalysts Comprised of Pd/C and H/La-BEA

Chen Zhao, Wenji Song, and Johannes A. Lercher*

Catalysis Research Center and Department of Chemistry, Technische Universität München, Garching 85747, Germany

Supporting Information

ABSTRACT: Aqueous phase catalytic phenol hydroalkylation and hydrodeoxygenation have been explored using Pd/C combined with zeolite H-BEA and La-BEA catalysts in the presence of H_2. The individual steps of phenol hydrogenation, cyclohexanol dehydration, or alkylation with phenol were individually investigated to gain insight into the relative rates in the cascade reactions of phenol hydroalkylation. The hydroalkylation rate, determined by the concentrations of phenol and cyclohexanol in phenol hydroalkylation, required the hydrogenation rate to be relatively slow. The optimized H^+/Pd ratio was 21, which allowed achieving comparable cyclohexanol formation rates via phenol hydrogenation and consumption rates from alkylation with phenol in phenol hydroalkylation. La-BEA was shown to be more selective for hydroalkylation than H-BEA in combination with Pd/C, because cyclohexanol dehydration was retarded selectively compared to alkylation of phenol. This indicates that dehydration is solely catalyzed by Brønsted acid sites, while alkylation can be achieved in the presence of La^{3+} cations.

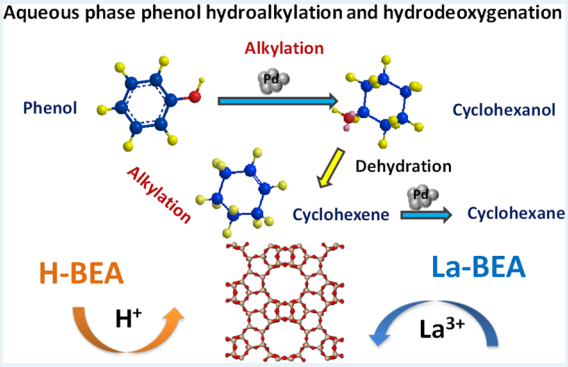

KEYWORDS: *phenol, hydroalkylation, deoxygenation, hydrogenation, sustainable chemistry*

1. INTRODUCTION

Selective transformation of lignocellulosic biomass into hydrocarbons that are suitable to be directly blended into liquid transportation fuels has been identified as one of the important targets in the conversion of bioderived raw materials.[1] In that context bifunctional catalysts containing metal and acid sites have been developed to convert lignin and cellulose derived phenols, aldehydes, alcohols, and furans to C_5−C_9 hydrocarbons.[2−11] However, it would be interesting to be able to selectively produce heavier (diesel range) hydrocarbons from lignocellulosic biomass.

Recently we reported in that context a novel route to aqueous phase hydroalkylation and deoxygenation of lignin derived C_6−C_9 phenolic oil to C_{12}−C_{18} hydrocarbons over Pd/C and zeolite H-BEA catalysts.[7] In the previous work, a detailed study of individual reactions of (substituted) phenol and their potential products (cyclohexanol, cyclohexanone, and cyclohexene) demonstrates that phenol selectively reacts with the in situ generated cyclohexanol or cyclohexene on Brønsted acid sites. The selectivity for phenol hydroalkylation depends on the concentrations of phenol and in situ formed cyclohexanol from phenol hydrogenation, as well as on the ratio of phenol to cyclohexanol determined by the rate of hydrogenation and the extent of reaction.

The presence of La^{3+} cation in zeolites has been reported to have positive effects ranging from stabilizing the zeolite against dealumination, modifying acid strength, and uniquely enhancing hydride transfer reactions, which have been found to be important for alkylation reactions.[12,13] Indeed, partially La^{3+} exchanged BEA and X type zeolites have shown high activity for carbon−carbon coupling reactions such as Friedel−Crafts acylation[14] and alkylation.[15]

In our quest to enhance the selectivity for hydroalkylation we compare, therefore, the catalytic properties of H-BEA and La-BEA in the presence of Pd/C in the aqueous phase. The individual kinetics of the aqueous phase dehydration, alkylation, and hydroalkylation−deoxygenation reactions of phenol are explored. In addition, an extensive characterization on these two zeolites was performed to elucidate the relationship between the catalyst properties and catalytic activities including their deactivation during hydroalkylation−deoxygenation of phenol.

2. EXPERIMENTAL SECTION

2.1. Chemicals. Zeolite H-BEA (H-form, Si/Al = 75, Süd Chemie AG München), Pd/C (5 wt % loading, Sigma-Aldrich), $La(NO_3)_3$ (Sigma-Aldrich, purity >99%), phenol (Sigma-Aldrich, 99.5%), cyclohexanone (Sigma-Aldrich, 99%), cyclohexanol (Sigma-Aldrich, 99%), ethyl acetate (Sigma-Aldrich, >99%), NH_3 (Air Liquide, >99.999%), N_2 (Air Liquide, >99.999%), He (Air Liquide, >99.999%), and H_2 (Air Liquide, >99.999%).

2.2. Ion Exchange Procedure for Preparing La-BEA Catalyst. Zeolite H-BEA (H-form) was ion-exchanged in 200

Received: June 29, 2012
Revised: September 14, 2012
Published: October 19, 2012

   dx.doi.org/10.1021/cs300418a | ACS Catal. 2012, 2, 2714−2723

mL of 0.2 M $La(NO_3)_3$ solution at 343 K for 2 h with stirring. Then, the exchanged zeolite was washed five times with 100 mL of deionized water and dried at 393 K for 12 h. Washed La-BEA was calcined in air (flow rate 100 mL·min^{-1}) at 723 K for 1 h with a heating rate of 2 K·min^{-1}. This ion exchange procedure was repeated three times.

2.3. Catalyst Characterization. Atomic absorption spectroscopy (AAS) for chemical analysis was performed on a UNICAM 939 AA spectrometer. N_2 adsorption−desorption was carried out at 77 K using a PMI automatic BET Sorptometer. Scanning electron microscopy (SEM) was recorded on a JEOL 500 SEM microscope. X-ray diffraction (XRD) patterns were recorded with a Philips X'Pert Pro System (Cu Kα, 0.1540 nm) operated at 40 kV/40 mA, in the range 2θ = 5−70° with a step size of 0.05° min^{-1}. The lanthanum concentration was determined by inductively coupled plasma (ICP) optical emission spectrometry with an FTMOA81A ICP-OES from Spectro-Analytical Instrument. Calibrating standards with 0, 10, 50, 75, and 100 ppm were prepared with lanthanum standard in a 5% w/w nitric acid solution.

The ^{27}Al and ^{29}Si MAS NMR spectra were recorded on a Bruker AV500 spectrometer. For ^{27}Al MAS NMR measurements, the samples were hydrated for three nights in a desiccator containing a beaker with water. Spectra measured were the sum of 2400 sweeps with a recycle time of 250 ms. The chemical shifts were referenced using an external standard of solid $Al(NO_3)_3$ (δ = −0.54 ppm). The ^{29}Si MAS NMR spectra recorded were the sum of at least 10 000 sweeps with a recycle time of 5 s. The excitation pulse had a length of 1.2 μs. The spectra were referenced to tetrakis(trimethylsilyl)silane (δ = −9.843 ppm). All NMR spectra were fitted with Gaussian functions for quantitative deconvolution of overlapping peaks.

Temperature programmed desorption of NH_3 (TPD-NH_3) was monitored under flow conditions. First the catalysts were activated in He at 623 K for 1 h using a heating rate of 5 K·min^{-1} from ambient temperature to 623 K. NH_3 was then adsorbed from 10 vol % in the He carrier gas (total flow 30 mL·min^{-1}, p = 30 mbar) at 373 K. The sample was purged with He for 2 h to remove physisorbed NH_3. Desorbing NH_3 was monitored by mass spectrometry (MS; Balzers QME 200).

The IR spectra of adsorbed pyridine were recorded on a Perkin-Elmer 2000 spectrometer operating at a resolution of 4 cm^{-1}. The catalyst samples were activated in a vacuum (p = 10^{-6} mbar) at 673 K for 1 h and then exposed to pyridine (p_{Py} = 10^{-1} mbar) at 423 K for 0.5 h. After evacuation at 423 K for 1 h, the spectra were recorded until equilibrium was achieved. IR spectra of adsorbed phenol or cyclohexanol were measured by the same procedure.

The matrix-assisted laser desorption/ionization (MALDI) time-of-flight mass spectra (TOF-MS) were recorded using a Bruker Biflex III MALDI-TOF mass spectrometer equipped with an N_2 laser (ν = 337 nm) ionization source operating at a pulse rate of 3 Hz. The ions were accelerated with pulsed-ion extraction after a delay of 50 ns at a voltage of 28.5 kV. The microchannel plate detector was operated in reflection mode. The mass spectrometer was calibrated with a polystyrene standard.

2.4. Catalytic Reactions. *2.4.1. Cyclohexanol Dehydration, Cyclohexanol−Phenol Alkylation, and Phenol Hydroalkylation−Deoxygenation.* Typically, a mixture of phenol (15 g), H_2O (80 mL), Pd/C (5 wt % Pd, 0.040 g), and H-BEA (0.20 g, Si/Al = 75) was loaded into an autoclave (Parr Instrument Co., 300 mL). The reactor with a stirring rate of 680 rpm was flushed with H_2 three times, subsequently the temperature was increased to 473 K, and 6 MPa H_2 was introduced at 473 K. The reactor was sampled after quenching with ice to ambient temperature, and organic products were extracted by ethyl acetate. The organic and aqueous phases were both analyzed by gas chromatography (GC; Shimadzu 2010, flame ionization detector) with a HP-5 capillary column (30 m × 250 μm) and a gas chromatography−mass spectrometry combination (GC−MS; Shimadzu QP 2010S). The carbon balance was better than 93 ± 3%. As this was a two-phase reaction, real-time sampling was difficult. The conversion/selectivity data were measured in separate experiments with varying duration times. The calculations of conversion and selectivity were based on a carbon mole basis, for which the terms are defined as follows: conversion = (starting material loss/initial charge)(100%); selectivity = (C atoms in each product/total C atoms in the products)(100%).

2.4.2. Catalyst Recycling Test. Catalyst stability was tested by recovering and reusing the catalyst charge as follows. A mixture of phenol (20 g), H-BEA or La-BEA (0.4 g), Pd/C (0.080 g), and H_2O (80 mL) was loaded into the Parr autoclave (300 mL). Reaction was conducted at 473 K and 6 MPa H_2 at a stirring speed of 700 rpm for 0.5 h. The reaction was quenched in ice, and the catalyst was separated from the aqueous phase by centrifugation, washed with acetone and water, dried in air at 383 K overnight, and reused in the next run. The catalyst recoveries were higher than 90 wt %. Four recycling runs were conducted in the present work.

3. RESULTS AND DISCUSSION

3.1. Catalyst Characteristics. This work uses as metal catalyst Pd/C and as acid catalysts H-BEA and La-BEA. The characteristics of Pd/C are compiled in the Supporting Information with the information of N_2 sorption, AAS, XRD, SEM, and TEM. Pd/C catalysts had a metal loading of 5 wt % and BET surface area of 1062 m^2·g^{-1} with a pore volume of 0.54 cm^3·g^{-1} and a mean pore diameter of 3.7 nm (Table S1 in the Supporting Information). The Pd^0 particle size of this catalyst was ca. 2.3 nm, calculated from a TEM image. The characteristics of acidic zeolites of H-BEA and La-BEA are described below.

3.1.1. Characterization of Texture and Morphology of BEA Catalysts. The results of the physicochemical characterization of H-BEA and La-BEA are compiled in Table 1. La-BEA was obtained from the exchange of H-BEA with $La(NO_3)_3$ three times at 343 K, and the La content in La-BEA was 1.22 wt % measured by ICP. The framework Si/Al ratios of H-BEA and La-BEA were 64 and 70, respectively, which indicates that dealumination occurred during the cation exchange and calcination process. The BET surface areas of H-BEA and La-BEA were comparable at 684 and 628 m^2·g^{-1}, respectively, with pore volumes of 0.43 and 0.40 cm^3·g^{-1} at pore diameters of 3.6 nm.

The SEM images of La-BEA and H-BEA show similar particles with an average size of 0.3 μm (Figure 1), implying that the particle size did not change during the cation exchange process. However, the partial loss of crystallinity upon La^{3+} cation exchange was detected by X-ray diffraction (XRD) (Figure 2). The strong reflections of La-BEA at 2θ of 7.5 and 22.5° were dramatically decreased compared to H-BEA. This indicates that the ion exchange and calcination procedures led to a partial loss of crystallinity of BEA.

dx.doi.org/10.1021/cs300418a | ACS Catal. 2012, 2, 2714−2723

Table 1. Elemental Compositions, BET Surface Areas, and Pore Volumes of H-BEA and La-BEA

	H-BEA	La-BEA
element composition (wt %)		
Si (AAS)	39.9	41.5
Al (AAS)	0.602	0.574
Na (AAS)	0.002	0.002
La (ICP)	–	1.22
Si/Al ($mol \cdot mol^{-1}$)	64	70
BET surface area ($m^2 \cdot g^{-1}$)	684	628
mesopore surface area ($m^2 \cdot g^{-1}$)	140	138
micropore surface area ($m^2 \cdot g^{-1}$)	544	490
pore volume ($cm^3 \cdot g^{-1}$)	0.43	0.40
mesopore volume ($cm^3 \cdot g^{-1}$)	0.21	0.20
micropore volume ($cm^3 \cdot g^{-1}$)	0.22	0.20
mean pore diameter (nm)	3.6	3.6

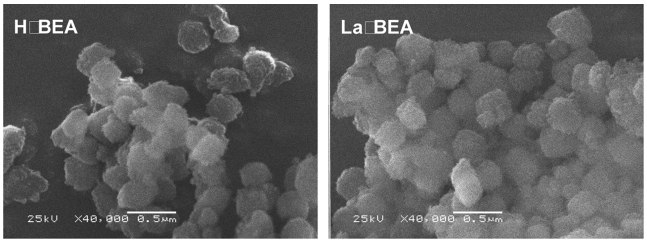

Figure 1. SEM images of H-BEA and La-BEA catalysts.

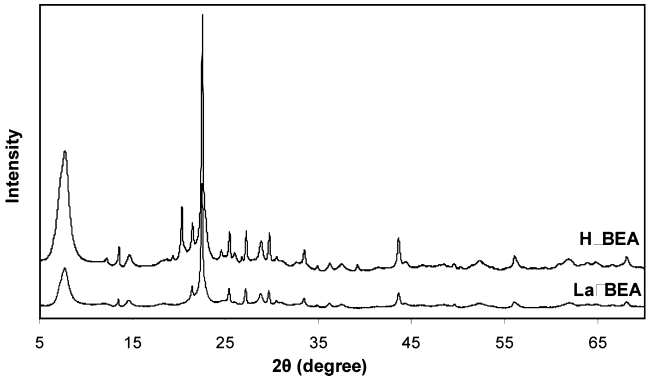

Figure 2. XRD patterns of H-BEA and La-BEA catalysts.

3.1.2. Characterization of Acid Sites of BEA Catalysts. The distributions and concentrations of acid sites were measured by temperature programmed desorption of NH_3 (TPD-NH_3). The maximum NH_3 desorption from the H-BEA and La-BEA zeolites appeared at 553 and 573 K, respectively (Figure 3a). The acid concentrations on H-BEA and La-BEA from TPD-NH_3 were 0.280 and 0.131 $mmol \cdot g^{-1}$, respectively (Table 1). Acid sites were also probed by IR spectroscopy of adsorbed pyridine (Py-IR; Figure 3b). The concentrations of Brønsted acid sites (BAS) and Lewis acid sites (LAS) were determined from the IR absorption bands at 1550 and 1450 cm^{-1}, respectively. The measured LAS concentrations for H-BEA and La-BEA were comparable at 0.066 and 0.065 $mmol \cdot g^{-1}$ (Table 1), but the BAS of H-BEA (0.201 $mmol \cdot g^{-1}$) was almost 4 times as high as that of La-BEA (0.058 $mmol \cdot g^{-1}$). The sums of acid concentrations from TPD-NH_3 were 10% higher than those determined by IR spectroscopy of adsorbed pyridine (Table 2), attributed to differences in the sampling techniques.

Table 2. Acid Site Concentrations of Phenol and Cyclohexanol on H-BEA and La-BEA

acid sites	H-BEA	La-BEA
acidity (Py-IR) ($mmol \cdot g^{-1}$)	0.267	0.123
Brønsted acid sites (BAS) ($mmol \cdot g^{-1}$)	0.201	0.058
Lewis acid sites (LAS) ($mmol \cdot g^{-1}$)	0.066	0.065
acidity (TPD-NH_3) ($mmol \cdot g^{-1}$)	0.280	0.131

3.1.3. Characterization of Framework Structure of BEA Catalysts. The ^{29}Si MAS NMR spectra of H-BEA and La-BEA (Figure 4a) show six peaks from Si atoms with zero to four nearest Al atoms. The fitting parameters of the ^{29}Si NMR spectra of hydrated H-BEA and La-BEA are compiled in Table 3. Based on Loewenstein's rule, Si/Al ratios in the framework of zeolite were determined to be 60 and 62 for H-BEA and La-BEA catalysts, respectively, which agrees well with the AAS results indicating Si/Al ratios of 64 and 70, respectively.

The local environments of the Al atoms in H-BEA and La-BEA were investigated by ^{27}Al MAS NMR spectroscopy (Figure 4b). The overlapping peaks at 53 and 57 ppm (from both H-BEA and La-BEA) are attributed to tetrahedrally coordinated Al (T_d Al) in the zeolite framework with protons or La^{3+} as charge compensating cations, respectively. The peak H-BEA at 0 ppm is assigned to octahedrally coordinated Al (O_h Al), present as extraframework species. The fitting results are compiled in Table 4, and the decreasing octahedral aluminum concentration from H-BEA (0.008 $mmol \cdot g^{-1}$) to La-BEA (0 $mmol \cdot g^{-1}$) indicates that dealumination occurred during the

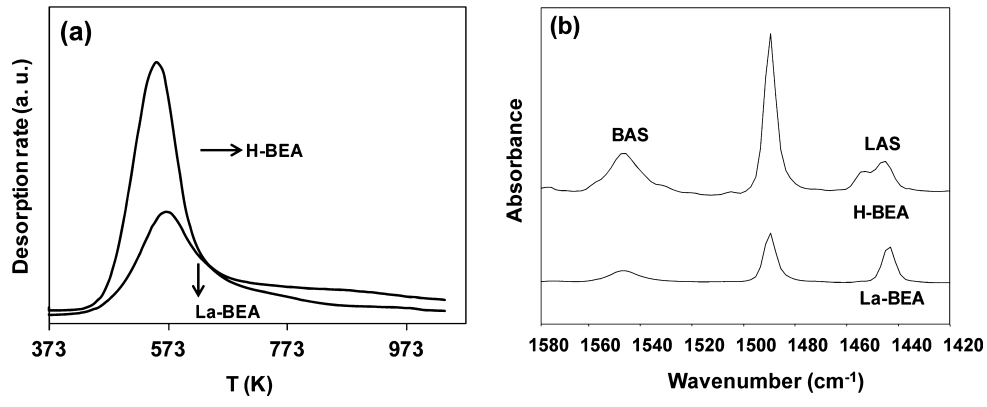

Figure 3. (a) Temperature programmed desorption of ammonia and (b) IR spectra of adsorbed pyridine on H-BEA and La-BEA catalysts.

dx.doi.org/10.1021/cs300418a | ACS Catal. 2012, 2, 2714–2723

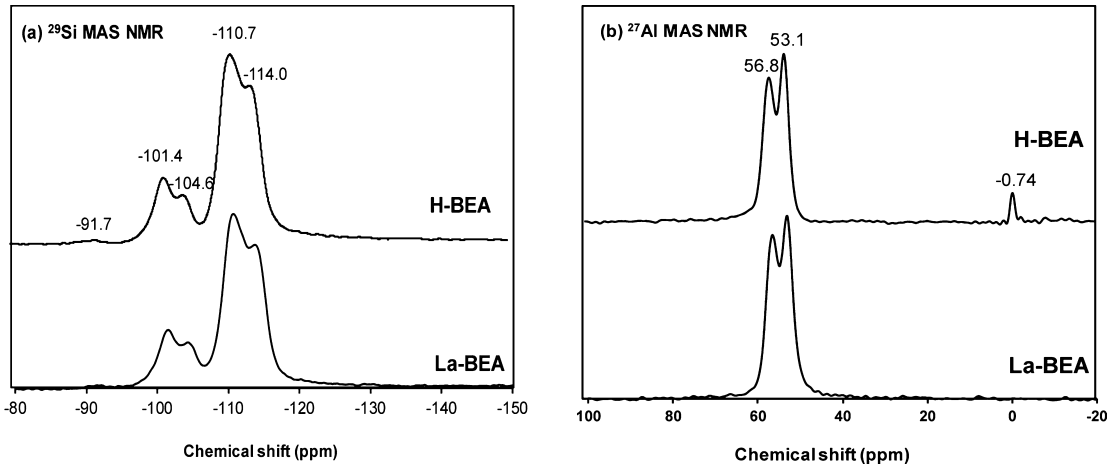

Figure 4. (a) ^{29}Si and (b) ^{27}Al MAS NMR spectra of H-BEA and La-BEA.

Table 3. Fitting Parameters of the ^{29}Si MAS NMR Spectra of H-BEA and La-BEA

	H-BEA			La-BEA		
Si (*n*Al)	chemical shift (ppm)	line width (ppm)	relative area (%)	chemical shift (ppm)	line width (ppm)	relative area (%)
n = 3	−91.7	0.7	0.06	−91.7	1.4	0.2
n = 1	−101.4	2.6	6.6	−101.4	2.6	6.4
n = 0	−104.6	2.2	4.6	−104.6	2.3	4.0
	−110.7	2.7	39.2	−110.7	2.8	39.9
	−113.9	2.7	28.8	−111.4	18.8	25.7
	−114.8	19.8	20.8	−114.0	2.6	26.5

Table 4. Fitting Parameters of the ^{27}Al MAS NMR Spectra of Hydrated H-BEA and La-BEA

	H-BEA			
assignment	δ (ppm)	QCC (MHz)	relative area (%)	concn[a] (mmol·g^{-1})
Td Al^{3+} close to H$^+$	56.8	3.0	51.3	0.114
	53.1	2.4	45.2	0.100
separate EFAL phase[b]	−0.74	1.0	3.5	0.008
	La-BEA			
assignment	δ (ppm)	QCC (MHz)	relative area (%)	concn[a] (mmol·g^{-1})
Td Al^{3+} close to H$^+$	56.8	2.7	44.5	0.095
Td Al^{3+} close to La^{3+}	53.1	3.1	55.5	0.118
separate EFAL phase[b]	–	–	–	–

[a]Based on the total Al concentration as determined by AAS. [b]Separate extraframework Al phase.

calcination after ion exchange in the aqueous solution. In particular it is noteworthy that all extralattice octahedral aluminum has been removed from the zeolite material. In comparison, the AAS results (shown in Table 1) showed that La-BEA lost 0.010 mmol·g^{-1} Al from the ion exchange treatment on H-BEA. The concentration of T_d aluminum in the lattice was slightly lower than the acid site concentration measured by IR spectroscopy of adsorbed pyridine, i.e., 0.214 mmol·g^{-1} from ^{27}Al MAS NMR and 0.267 mmol·g^{-1} from Py-IR for H-BEA, as well as 0.095 and 0.123 mmol·g^{-1} from ^{27}Al MAS NMR and Py-IR for La-BEA, respectively. This indicates that weak Brønsted acid sites such as silanol nests generated by dealumination should contribute to the overall Brønsted acid site concentration.

3.1.4. Characterization of Adsorption Properties of BEA Catalysts. The adsorption properties of H-BEA and La-BEA were investigated in the presence of 0.5 mbar of gas phase organic reactants at 313 K (Figure 5). La-BEA had triple the capacity of H-BEA for adsorption of phenol (at the representative adsorption of 1610 cm^{-1}) at these conditions (Figure 5a). This suggests that alkaline La^{3+} cations adsorbed acidic phenol more strongly than acidic protons did. The adsorption capacities for cyclohexanol (at the representative adsorption of 2950 cm^{-1}), however, were equal on La-BEA and H-BEA (Figure 5b). In general, the intrinsic properties of La-BEA led to much higher adsorption of the reactant phenol and intermediate cyclohexanol.

3.2. Catalytic Reaction Measurements. *3.2.1. Kinetics of Cyclohexanol Dehydration on H-BEA and La-BEA.* Cyclohexanol dehydration in liquid water catalyzed by H-BEA or La-BEA yielding only cyclohexene was measured with a very high substrate to catalyst ratio in batch mode at 473 K as a function of time (Figure 6). To use conditions analogous to hydroalkylation, hydrogen (4 MPa H_2) was introduced to each experiment before reaction. Cyclohexanol conversion to cyclohexene increased linearly with time (Figure 6), showing that the catalysts did not deactivate. The dehydration rate was 5 times higher with H-BEA (0.23 mol·g^{-1}·h^{-1}) than with La-BEA (0.045 mol·g^{-1}·h^{-1}) (Table 5). In our previous work, we showed that the BAS of HZSM-5 are the primary active sites for dehydration in the aqueous phase.[5,16] The dehydration TOFs (per mole of converted reactant on per mole of active sites (BAS) per hour) on H-BEA and La-BEA were 1142 and 776 mol·mol$_{BAS}^{-1}$·h^{-1}, respectively, indicating that the introduction of La^{3+} moderately reduced the specific activity of the residual Brønsted acid sites.

3.2.2. Kinetics of Phenol–Cyclohexanol Alkylation on H-BEA and La-BEA. The alkylation of phenol and cyclohexanol (1:1 molar ratio) was conducted in the aqueous phase using H-BEA and La-BEA at 473 K (Figure 7). Two product groups were observed, i.e., cyclohexene, which was the dominating product, and 2- and 4-cyclohexylphenols, the products of alkylation. Both product groups approach equilibrium levels under the conditions measured; thus only the early stages of the reaction will be discussed.

dx.doi.org/10.1021/cs300418a | ACS Catal. 2012, 2, 2714–2723

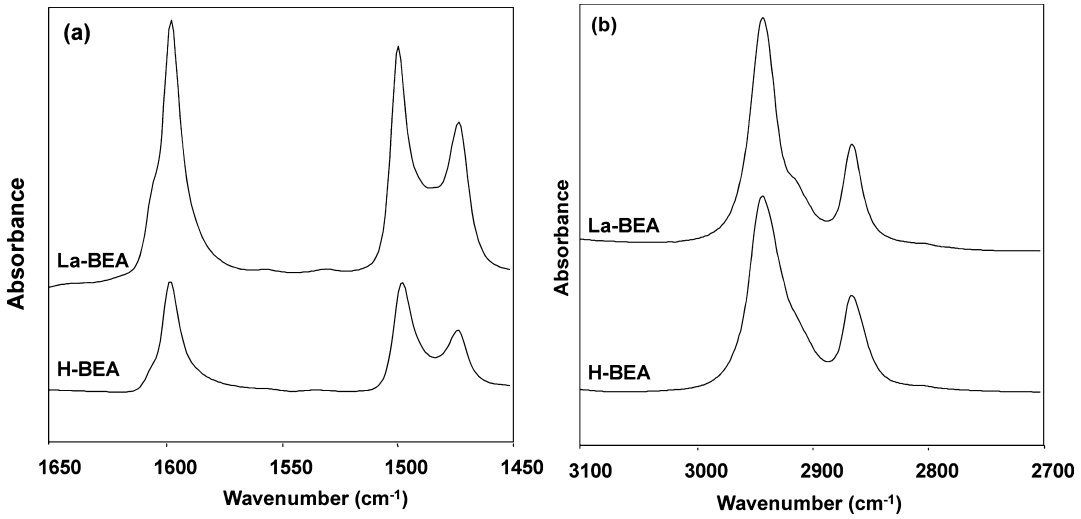

Figure 5. IR spectra of adsorbed (a) phenol and (b) cyclohexanol on H-BEA and La-BEA from the gas phase at 313 K (p = 0.5 mbar).

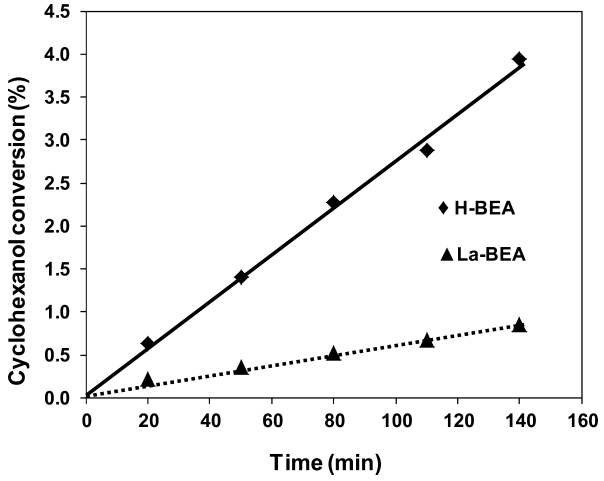

Figure 6. Cyclohexanol conversion with H-BEA (solid line) and La-BEA (dashed line) as a function of time. Reaction conditions: cyclohexanol (60 g), catalyst (0.040 g), H_2O (80 mL), 473 K, 4 MPa H_2 (ambient temperature), and stirring at 700 rpm.

Table 5. Initial Rates of Hydrogenation of Phenol on Pd/C[3] and Initial Rates of Dehydration, Alkylation, and Hydroalkylation of Cyclohexanol and Phenol on H-BEA and La-BEA

(a) Initial Rates of Hydrogenation of Phenol on Pd/C[3]	
reaction	Pd/C
hydrogenation of phenol to cyclohexanone on Pd/C (r_1)	
rate ($mol \cdot g^{-1} \cdot h^{-1}$)	1.0
TOF ($mol \cdot mol_{Pd\ surf.}^{-1} \cdot h^{-1}$)	4200
hydrogenation of cyclohexanone to cyclohexanol on Pd/C (r_2)	
rate ($mol \cdot g^{-1} \cdot h^{-1}$)	5.1
TOF ($mol \cdot mol_{Pd\ surf.}^{-1} \cdot h^{-1}$)	21000

(b) Initial Rates of Dehydration, Alkylation, and Hydroalkylation of Cyclohexanol and Phenol on H-BEA and La-BEA		
reaction	H-BEA	La-BEA
dehydration of cyclohexanol on BEA (r_3)		
rate ($mol \cdot g^{-1} \cdot h^{-1}$)	0.23	0.045
TOF ($mol \cdot mol_{BAS}^{-1} \cdot h^{-1}$)	1142	776
alkylation of phenol and cyclohexanol on BEA (r_4)		
$rate_{alkylation}$ ($mol_{alkylation} \cdot g^{-1} \cdot h^{-1}$)	0.036	0.033
$TOF_{alkylation}$ ($mol_{alkylation} \cdot mol_{BAS}^{-1} \cdot h^{-1}$)	1791	5690
hydroalkylation of phenol with acid and Pd/C		
rate ($mol_{alkylation} \cdot g^{-1} \cdot h^{-1}$)	0.034	0.046

The negligible selectivity to alkylated products at initial conversions indicates that alkylation proceeds firstly via cyclohexanol dehydration to cyclohexene (see Figure 7b and Scheme 1). The cyclohexanol and phenol conversions were 88 and 20%, respectively, with H-BEA or La-BEA catalysts after reaching the dehydration and alkylation equilibrium (reversible reaction) (Figure 7a). Thus, cyclohexanol was dehydrated to cyclohexene as a primary product, and alkylation occurred as a secondary reaction (Table 5). With time the cyclohexene selectivity decreased from 100 to 55%, as the cyclohexene was consumed in alkylation (Figure 7b). The yield of cyclohexene first increased to 65% over both catalysts and then decreased to 50% due to its further alkylation with phenol as the reaction time proceeded (see Figure 7c). The yields of alkylation products increased from 0 to 20% as the reaction time increased. The conversion rate and the selectivity toward alkylation were slightly higher in the case of H-BEA than with La-BEA, both reaching a value of 0.033 $mol \cdot g^{-1} \cdot h^{-1}$. It should be emphasized that the TOFs of alkylation were 1791 and 5690 $mol \cdot mol_{BAS}^{-1} \cdot h^{-1}$ for H-BEA and La-BEA, respectively, indicating a higher intrinsic activity in the presence of La^{3+} (see also Table 5).

3.2.3. Kinetics of Phenol Hydroalkylation–Deoxygenation on H-BEA and La-BEA in the Presence of Pd/C. When the Pd/C hydrogenation catalyst is combined with H-BEA or La-BEA (acting as solid acid), the conversion of phenol becomes more complex. Phenol can be hydrogenated to cyclohexanol (designated $r_1 + r_2$); then it is either dehydrated to cyclohexene, which is rapidly hydrogenated to cyclohexane (designated r_3), or alkylated with phenol to form 2- and 4-cyclohexylphenols (designated r_4). The latter compound or heavier alkylation products can be deoxygenated through dehydration and hydrogenation to form the final C_{12} and C_{18} cycloalkanes (Scheme 1).[7]

As shown in Figure 8a, the phenol conversion reached 60% and the alkylation yield reached 25% on both catalysts within 200 min. The initial product was cyclohexanol with 100% selectivity at t = 0 (Figure 8c), decreasing to 50% due to

dx.doi.org/10.1021/cs300418a | ACS Catal. 2012, 2, 2714–2723

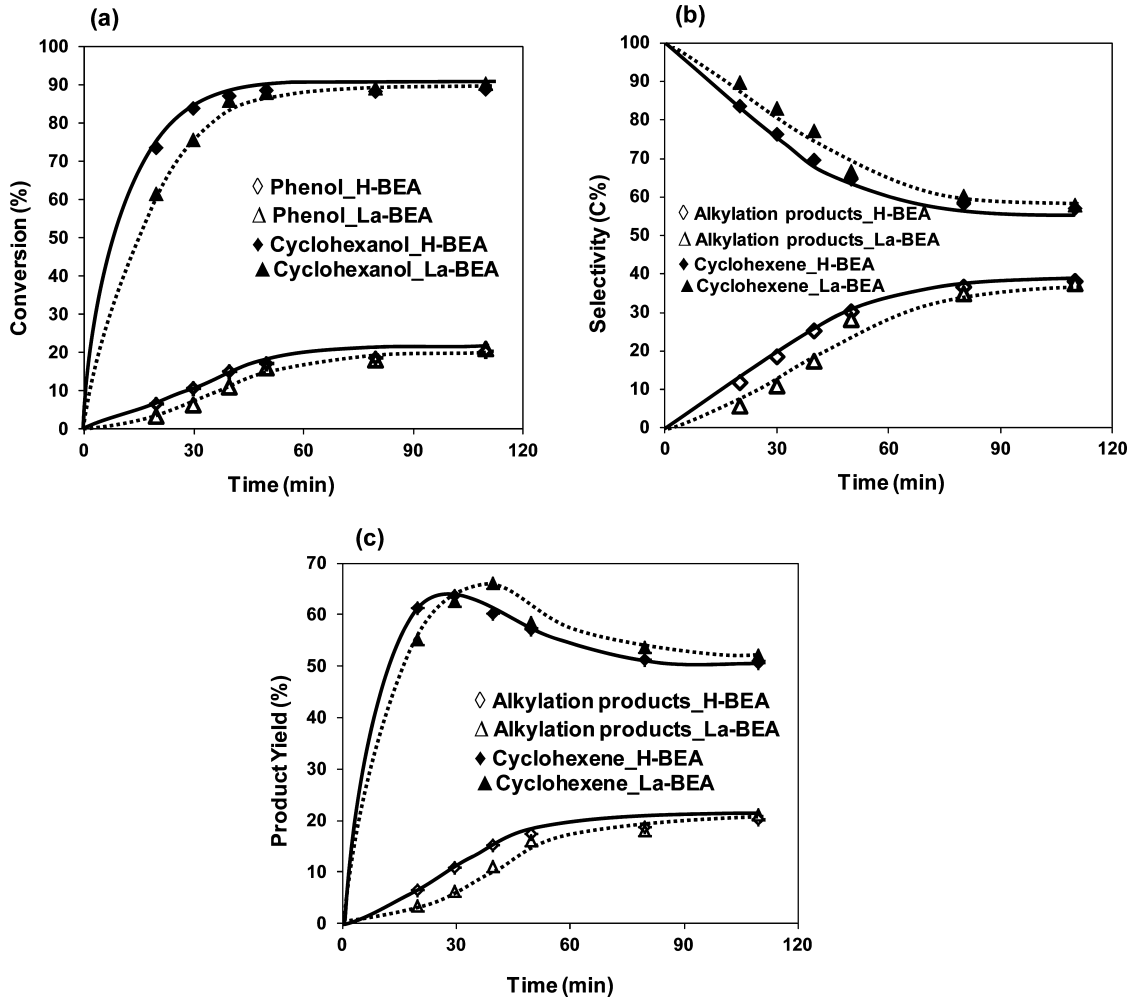

Figure 7. Product distribution from alkylation of phenol and cyclohexanol with H-BEA (solid line) or La-BEA (dashed line) as a function of time: (a) conversion, (b) selectivity, and (c) yield. Reaction conditions: phenol (15 g), cyclohexanol (15 g), catalyst (0.40 g), H_2O (80 mL), 473 K, 4 MPa H_2 (ambient temperature), and stirring at 700 rpm.

alkylation leading ultimately to bicyclohexane and tricyclohexane. As the alkylation rate (0.036 mol·g^{-1}·h^{-1}) was much slower than the hydrogenation rate (1.0 mol·g^{-1}·h^{-1}) in the presence of H-BEA (Table 5), alkylated phenol was not detected, but partially hydrogenated cyclohexyl-cyclohexanone (CCN) was the major product, increasing to 45% selectivity with increasing reaction time.

In addition, deoxygenated bicyclohexane and cyclohexyl trimer were observed with 1−3% selectivities from Pd/C and H-BEA or La-BEA catalysts. The hydroalkylation rates on La-BEA in the presence of Pd/C reached 0.046 mol$_{alkylation}$·g^{-1}·h^{-1}, which was higher than the rate with H-BEA (0.034 mol$_{alkylation}$·g^{-1}·h^{-1}). The hydrodeoxygenation selectivity to cyclohexane was lower than 1.5% (Figure 8c), indicating that the cyclohexanol intermediate is preferentially alkylated with phenol rather than being dehydrated (and hydrogenated).

3.2.4. Comparison of Initial Rates in the Coupled Reactions of Hydrogenation, Dehydration, Alkylation, and Hydroalkylation. Hydrogenation, dehydration, and alkylation proceed in tandem during phenol hydroalkylation over bifunctional catalysts. The initial rates are compiled in Table 5. The rates of hydrogenation of phenol and cyclohexanone over Pd/C were 1.0 and 5.1 mol·g^{-1}·h^{-1}, respectively. On H-BEA, the rate of dehydration of cyclohexanol was 0.23 mol·g^{-1}·h^{-1}, and the rate of alkylation of phenol by cyclohexanol was 0.036 mol·g^{-1}·h^{-1}. By comparison, the dehydration and alkylation rates in the presence of La-BEA were 0.045 and 0.033 mol·g^{-1}·h^{-1}, respectively. This result shows that though the isolated dehydration activity may be quite different, the alkylation activity is comparable on two BEA catalysts, suggesting that isolated dehydration is catalyzed by protons in BEA catalyst without a significant effect of the presence of La^{3+}, but that the alkylation activity of Brønsted acid sites is enhanced by La^{3+}.

In the phenol hydroalkylation with Pd/C and H-BEA or La-BEA without cyclohexanol as a supplied co-reactant, hydrogenation controlled the concentration ratio of phenol to cyclohexanol reactants during the working conditions. The excess of phenol drove the alkylation if the hydrogenation conversion was slow. However, too slow hydrogenation conversion supplied insufficient cyclohexanol, resulting in even lower alkylation rates. Therefore, the ratio of metal sites catalyzing hydrogenation to acid sites catalyzing dehydration and alkylation has to be optimized. In a previous report, only Pd showed high phenol hydroalkylation selectivity in the presence of H-BEA in water.[7] Other metals such as Pt, Ru, Rh, and Ni directly catalyzed cyclohexane formation from phenol through hydrogenation−dehydration. The slow alkylation

dx.doi.org/10.1021/cs300418a | *ACS Catal.* 2012, 2, 2714−2723

Scheme 1. Proposed Pathways for Dehydration of Cyclohexanol, Alkylation of Phenol and Cyclohexanol, and Hydroalkylation of Phenol in Aqueous Phase

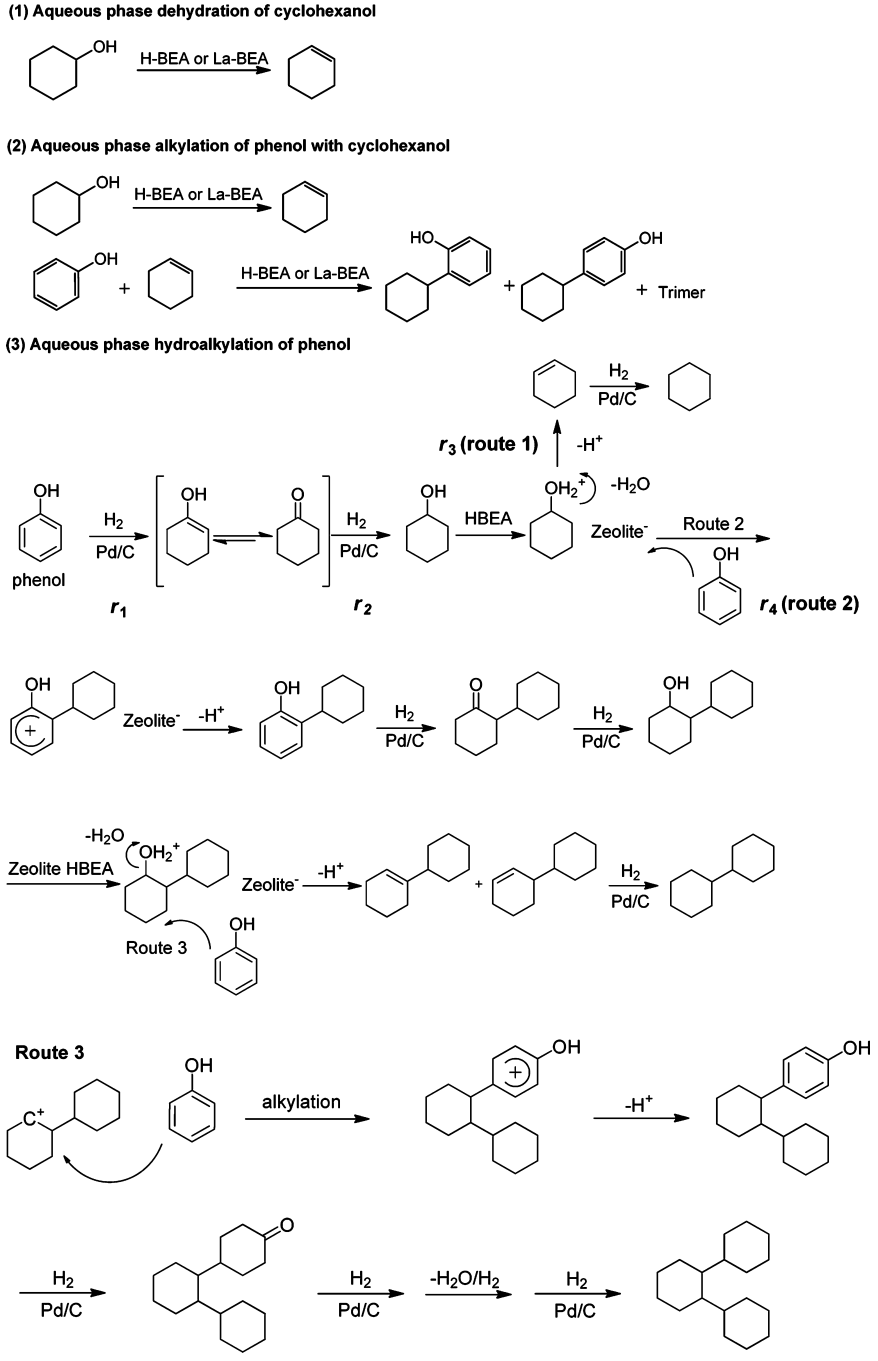

reaction requires a long contact time for the alkylating molecules to achieve high conversion. The Pd hydrogenation catalyst that sustains a high concentration of the cyclohexanone intermediate enables a relatively higher rate of alkylation. In our previous contribution,[7] the optimized phenol/Pd ratios were in the range 2254−4508 mol/mol at 473 K, attaining 67−85% yields of alkylation products. When the phenol/Pd ratio was lowered to 564 mol/mol, the dominant product was cyclohexane (yield 98%). On the basis of the calculated individual hydrogenation rates on phenol and cyclohexanone over Pd/C (see Table 5), it can be estimated that after 0.5 h the ratio of phenol/cyclohexanol was ca. 9:1, if the phenol/Pd ratio was 2254 (0.040 g of 5 wt % Pd/C and 4.0 g of phenol). Such a high ratio of phenol to cyclohexanol during the conversion would enhance the alkylation efficiency in phenol self-hydroalkylation.

Subsequent to phenol hydrogenation, the dehydration and alkylation of cyclohexanol took place in parallel. In a previous study,[7] we have concluded that H-BEA with a high concentration of Brønsted acid sites such as H-BEA 25 (Si/Al = 12.5) was more selective to alkene formation, but H-BEA 150 (Si/Al = 75) favored a higher alkylation selectivity.

In addition, the ratio of metal to acid sites was also crucial for determining the product distribution; that is, a very small amount of H-BEA (0.1 g, in the presence of 0.04 g of 5 wt % Pd/C) was ineffective for cyclohexanol dehydration at 433 K,

dx.doi.org/10.1021/cs300418a | ACS Catal. 2012, 2, 2714−2723

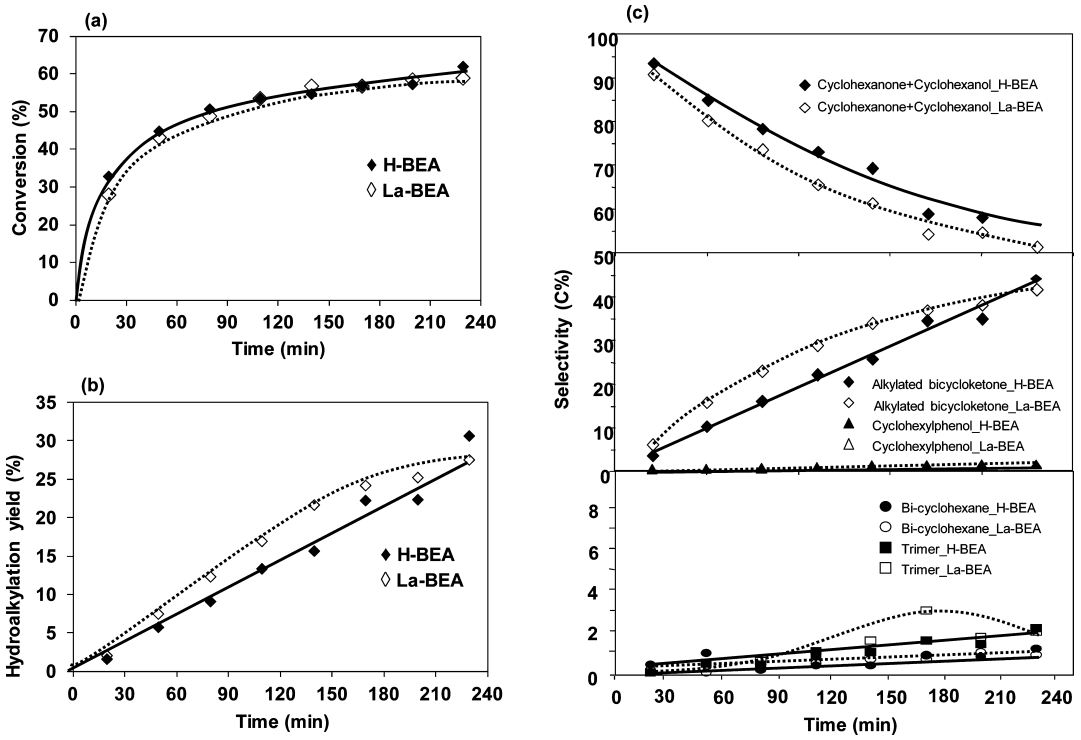

Figure 8. Product distributions from phenol hydroalkylation with Pd/C and H-BEA (solid line) or La-BEA (dashed line) as a function of time. Reaction conditions: phenol (15 g), solid acid (0.20 g), Pd/C (0.040 g), H_2O (80 mL), 473 K, 4 MPa H_2 (ambient temperature), stirring at 700 rpm.

Scheme 2. Reaction Sequence for Phenol Hydroalkylation Including Hydrogenation, Dehydration, and Alkylation Elementary Steps

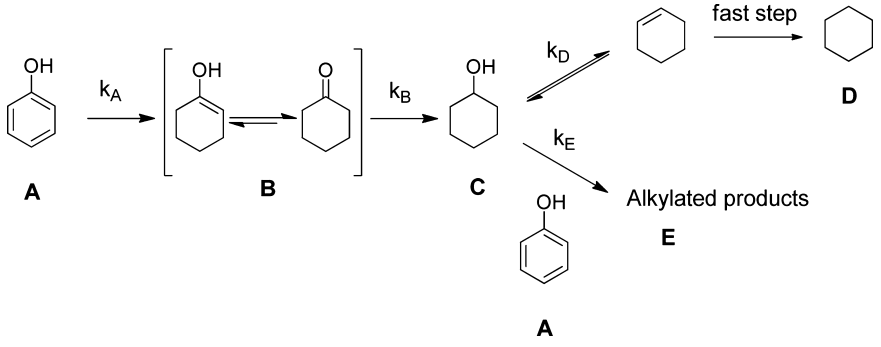

but the increasingly added concentrations of H-BEA 150 (0.1−1.0 g) preferred to dehydrate cyclohexanol (63% selectivity), and subsequently the added H-BEA 150 concentrations (1.0−2.0 g) took alkylation precedence over dehydration at attaining an alkylation selectivity of 36%. Therefore, in the previous study,[7] the optimized metal to acid ratio to enhance hydroalkylation selectivities, i.e., the Pd to H^+ ratio was 1/22 mol/mol, suggesting that acid sites are more abundant than metal sites in the dual function catalysts. The maximum productivity would be reached if the hydrogenated product, cyclohexanol, is quantitatively consumed as it is formed. On the basis of the individual rates one would estimate the ratio of Pd to H^+ to be 1/21, i.e., adjusting the alcohol formation rates from phenol with Pd/C (TOF = 5.1 $mol \cdot mol_{Pd\ surf.}^{-1} \cdot h^{-1}$) to match the rate of its consumption by alkylation (TOF = 1791 $mol_{alkylation} \cdot mol_{BAS}^{-1} \cdot h^{-1}$) with H-BEA (see Table 5). This matches well with the experimental ratio of 1/22.

In essence, if the alkylation selectivity with cyclohexanol needs to be enhanced, the dehydration rates should be retarded, as the dehydrated cyclohexene is swiftly and in part irreversibly converted to cyclohexane. The challenge lies in the fact that for the hydroalkylation of phenol both critical reactions are catalyzed by Brønsted acid sites. Hence, the specific activity of the alkylation function has to be enhanced and employing a catalyst selective to alkylation is crucial for determining the final product distribution. In a comparison, H-BEA shows higher dehydration rates, but catalyzes almost identical alkylation rates, compared to La-BEA. Thus, in the sequence of parallel dehydration and alkylation reactions, La-BEA delivers higher selectivity to alkylation. In addition, the higher adsorption of phenol and cyclohexanol on the surface of La-BEA (Figure 5) further increases the alkylation rates. The experimental results also support this hypothesis (Figure 8b,c), that La-BEA is more selective for hydroalkylation.

dx.doi.org/10.1021/cs300418a | *ACS Catal.* 2012, 2, 2714−2723

3.2.5. Fitting Phenol Hydroalkylation in the Kinetics Model. Scheme 2 simplifies the elementary reactions involved in the phenol hydroalkylation in the presence of dual functional catalysts. It starts with partial hydrogenation of phenol to cyclohexanone (referred to as "A"), which is formed from keto−enol tautomerism of cyclohexene-ol (referred to as "B"), and cyclohexanone can be fully hydrogenated to cyclohexanol (referred to as "C"). Cyclohexanol can be either dehydrated/hydrogenated to cyclohexane (referred to as "D") or alkylated with phenol (A) to heavier products (referred to as "E").

The differential kinetic rate equations involved in the phenol hydroalkylation are the following:

$$\frac{d[A]}{d\tau} = -k_A[A] - k_E[A][C]$$

$$\frac{d[B]}{d\tau} = -k_A[A] - k_B[B]$$

$$\frac{d[C]}{d\tau} = k_B[B] - k_D[C] - k_E[C]$$

$$\frac{d[D]}{d\tau} = k_D[C]$$

$$\frac{d[E]}{d\tau} = k_E[C][A]$$

The rate of consumption of A

$$-r_A = \frac{d[A]}{d\tau} = -k_A[A] - k_E[A][C]$$

has a unit of mol·h^{-1}, k is a rate constant with a unit of h^{-1}, and [A] is the concentration of phenol during the reaction. Table 6 displays the used apparent rate constants (the product of the true rate constant and the adsorption equilibrium constant of the reactant) for fitting phenol hydroalkylation with Pd/C, H-BEA, or La-BEA in the kinetic model (for reaction conditions, see Figure 8). The simulation results are in good agreement with the experimental data, suggesting that the proposed mechanism and kinetic model for phenol hydroalkylation and hydrodeoxygenation are reasonable. The fitted results (Figure 9) indicate that the concentration of reactant phenol (A) continuously decreases and the hydrogenated cyclohexanone and cyclohexanol (B + C) appear as the primary products, while alkylation (E) and hydrodeoxygenation products (D) occur as the secondary products. These fitted data show that k_A, k_B, and k_E are comparable but k_D on H-BEA is 4 times greater than that on La-BEA, while the BAS on H-BEA is consistently 4 times higher compared to that on La-BEA. Thus, it supports the hypothesis that the protons on BEA catalyze alcohol dehydration without a strong positive impact of La^{3+}, but that in the presence of La^{3+} the catalytic activity of Brønsted acid for alkylation is enhanced.

Table 6. Rate Constants Used for Fitting Phenol Hydroalkylation

	k_A (h^{-1})	k_B (h^{-1})	k_D (h^{-1})	k_E (h^{-1})
Pd/C, H-BEA	0.15	0.17	0.060	0.046
Pd/C, La-BEA	0.14	0.16	0.015	0.042

3.3. Catalyst Recycling Test. To test the catalyst stability for phenol hydroalkylation at the hydrothermal conditions used, the activities were examined in four consecutive catalytic runs employing the same aliquot of catalyst (Figure 10). The recycling data showed that the activities of used catalysts did not decrease during four catalytic runs, attaining ca. 40% conversions and selectivities of 20% hydroalkylation and 80% hydrodeoxygenation in each run. This result indicates that the combination of metal and acid catalysts had high activity and stability under hydrothermal conditions.

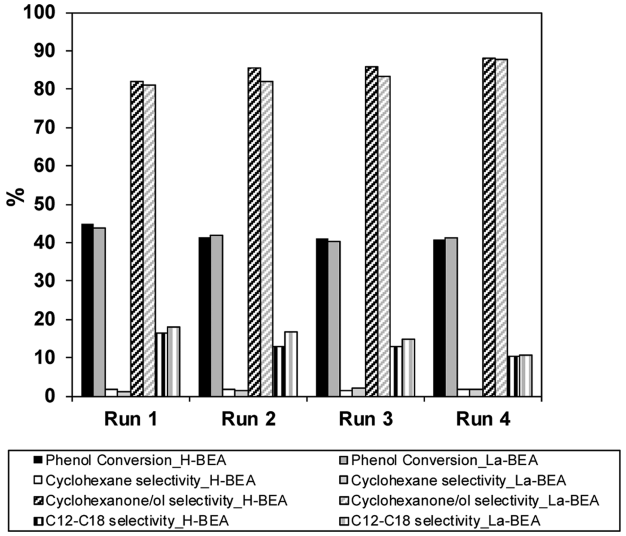

Figure 10. Catalytic recycling test with Pd/C and H-BEA or La-BEA for hydroalkylation of phenol. Reaction conditions: phenol (20 g), H-BEA or La-BEA (0.4 g), Pd/C (0.080 g), H_2O (80 mL), 473 K, 6 MPa H_2 (reaction temperature), 0.5 h, and stirring at 700 rpm.

After reaction the color of zeolites H-BEA and La-BEA had changed from white to orange. As the used zeolite was more

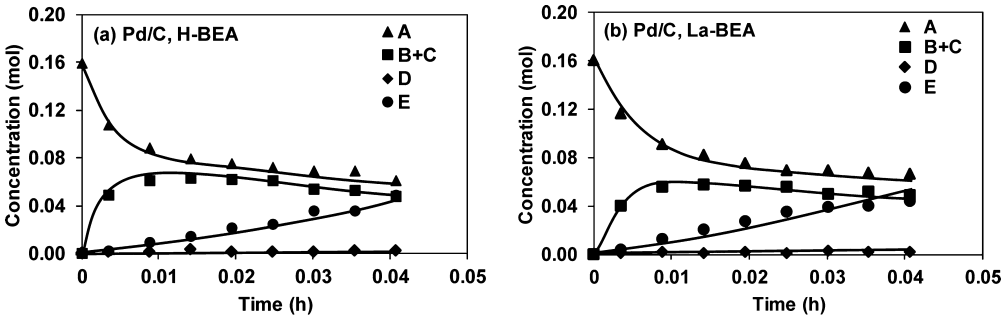

Figure 9. Kinetics from the experimental data (solid points) and fitted curves from the kinetics model (solid line).

dx.doi.org/10.1021/cs300418a | *ACS Catal.* 2012, 2, 2714−2723

abundant than Pd/C, the color of the Pd/C did not obscure the change of zeolite color. The yellow compounds were extracted into acetone and analyzed by MALDI-TOF mass spectrometry. The obtained MALDI-TOF-MS spectrum (Supporting Information) showed that the yellow compounds are likely an oligomeric product mixture such as the polyphenol nuclear compounds formed by bialkylation with phenol. The heavier compounds were formed in low amounts (carbon balance in the reaction exceeded 95%), and the nearly unchanged activities during the recycling (Figure 10) indicated that such polymers did not block the active sites for phenol hydroalkylation.

4. CONCLUSIONS

In the phenol hydroalkylation with catalysts Pd/C and H-BEA or La-BEA, hydrogenation, dehydration, and alkylation proceed together. The hydrogenation rate controls the ratio of alkylation reactants, i.e., phenol and cyclohexanol. A high ratio of phenol to cyclohexanol promotes the alkylation, which requires in turn the hydrogenation to be slow relative to the phenol concentrations. Additionally, the ratio of metal to acid sites, in the present case 1:21 Pd/H^+ for the combination of Pd/C and H-BEA, has to be adjusted to be able to attain comparable cyclohexanol formation rates from phenol hydrogenation and consumption rates from alkylation with phenol.

Following the phenol hydrogenation step, the subsequent dehydration/hydrogenation and alkylation of cyclohexanol compete. La-BEA was proved to be more selective for hydroalkylation, probably due to the dominant alkylation over dehydration in the cascade reactions. While La^{3+} does not exert a significant influence on Brønsted acid sites for dehydrogenation, it positively influences their catalytic activity for alkylation. The catalysts did not deactivate during four catalytic runs, suggesting that such catalyst combination is stable in hot water under selected conditions.

■ ASSOCIATED CONTENT

Supporting Information

Characterization of 5 wt % Pd/C by SEM, TEM, and XRD; surface area and pore volume information for Pd/C; MALDI-TOF-MS spectrum of the yellow compounds produced from phenol hydroalkylation with Pd/C and H-BEA catalysts. This material is available free of charge via the Internet at http://pubs.acs.org.

■ AUTHOR INFORMATION

Corresponding Author

*Tel.: (+)49-89-28913540. Fax: (+)49-89-28913544. E-mail: johannes.lercher@ch.tum.de.

Notes

The authors declare no competing financial interest.

■ ACKNOWLEDGMENTS

The work is supported by Technische Universität München in the framework of European Graduate School for Sustainable Energy.

■ REFERENCES

(1) Corma, A.; Iborra, S.; Velty, A. *Chem. Rev.* **2007**, *107*, 2411.
(2) Zhao, C.; Kou, Y.; Lemonidou, A. A.; Li, X.; Lercher, J. A. *Angew. Chem., Int. Ed.* **2009**, *48*, 3987.
(3) Zhao, C.; He, J.; Lemonidou, A. A.; Li, X.; Lercher, J. A. *J. Catal.* **2011**, *280*, 8.
(4) Zhao, C.; Kou, Y.; Lemonidou, A. A.; Li, X.; Lercher, J. A. *Chem. Commun.* **2011**, *46*, 412.
(5) Hong, D. Y.; Miller, S. J.; Agrawal, P. K.; Jones, C. W. *Chem. Commun.* **2010**, *46*, 1038.
(6) Zhao, C.; Lercher, J. A. *Angew. Chem., Int. Ed.* **2012**, *51*, 5935.
(7) Zhao, C.; Camaioni, D.; Lercher, J. A. *J. Catal.* **2012**, *288*, 92.
(8) Crossley, S.; Faria, J.; Shen, M.; Resasco, D. E. *Science* **2010**, *327*, 68.
(9) Sitthisa, S.; An, W.; Resasco, D. E. *J. Catal.* **2011**, *284*, 90.
(10) Zhu, X.; Lobban, L. L.; Mallinson, R. G.; Resasco, D. E. *J. Catal.* **2011**, *281*, 21.
(11) Vispute, T. P.; Zhang, H.; Sanna, A.; Xiao, R.; Huber, G. W. *Science* **2010**, *330*, 1222.
(12) Gaare, K.; Akporiaye, D. *J. Phys. Chem. B* **1997**, *101*, 48.
(13) Sievers, C.; Onda, A.; Olindo, R.; Lercher, J. A. *J. Phys. Chem. C* **2007**, *111*, 5454.
(14) Sheemol, V. N.; Tyagi, B.; Jasra, R. V. *J. Mol. Catal. A* **2004**, *215*, 201.
(15) Sievers, C.; Liebert, J. S.; Stratmann, M. M.; Olindo, R.; Lercher, J. A. *Appl. Catal., A: Gen.* **2008**, *336*, 89.
(16) Peng, B.; Zhao, C.; Mejía-Centeno, I.; Fuentes, G. A.; Jentys, A.; Lercher, J. A. *Catal. Today* **2012**, *183*, 3.